Parallel implementation of the equation-of-motion coupled-cluster singles and doubles method and application for radical adducts of cytosine

Tomasz Kuś,[a] Victor F. Lotrich, and Rodney J. Bartlett
Quantum Theory Project, Department of Chemistry, and Department of Physics, University of Florida, Gainesville, Florida 32611, USA

(Received 4 December 2008; accepted 9 February 2009; published online 31 March 2009)

The equation-of-motion coupled-cluster singles and doubles (EOM-CCSD) method has been implemented into the massively parallel ACES III program using two alternative strategies: (1) storing the entire EOM Hamiltonian matrix prior to diagonalization and (2) recomputing the four-virtual part of the matrix from integrals in a direct mode. The second is found to be far more efficient. EOM-CC shows virtually ideal scaling from 32 to 256 processors. With basis sets as large as 552 functions, the program was applied to determine vertical excitation energies for five cytosine radical adducts of –OH and –H at three sites C5, C6, and N3. These radicals are considered to play an important role in radiation induced DNA damage. The excitation energy spectrum shows two distinct patterns for the lowest transitions distinguishing the C6–OH, C6–H, and N3–H adducts from the C5–OH and C5–H. The results indicate that the two lowest transitions of the C6–OH isomer should contribute to the experimentally observed absorption maximum at 2.88 eV, while the third and fourth transitions of C6–OH and the two lowest transitions of C5–OH contribute to the 3.65 eV absorption maximum. We also report the CCSD with noniterative triples correction [CCSD(T)] relative energies of the C5–OH and C6–OH adducts using 1000 processors.
 [DOI: 10.1063/1.3091293]

I. INTRODUCTION

Radicals formed by radiation processes attack DNA, causing damage to occur during mutagenesis, carcinogenesis, and aging.[1–4] One of these radicals is OH, which damages DNA by its adduction to nucleobases. Another process leading to DNA degradation is connected with the formation of hydrogen adducts of nucleobases. The identification and elucidation of nucleobase radical formation are critical to understanding issues pertaining to radiation exposure of DNA.

The present work, to the best of our knowledge, is a first study of the equation-of-motion coupled-cluster (EOM-CC) method applied to open-shell derivatives of nucleobases. Previous EOM-CC applications studying this subject dealt with closed-shell systems.[5,6]

The ground state of cytosine OH adducts has been studied experimentally,[7–9] providing some information about the relative stability of the isomers. However little data have been provided about the excited state properties of the cytosine radicals, though there are experimental studies reporting the spectra of cytosine OH adducts.[10–12] Both the stability of the isomers and the assignment of the observed spectra are crucial for the identification of the isomer, which is required to assess the mechanism and extent of DNA damage. Since the experimental investigations cannot fully explain the problem, theoretical results become a valuable source of information.[13–16] Theoretical studies are even more important for the H cytosine adduct since there are only a limited number of experimental studies.[17–19] Some of the issues concerning hydrogen adducts can be found in the literature.[15,19–22]

The ground state equilibrium structures are determined at the second-order many-body perturbation-theory [MBPT(2)] level. The electronic structure of the ground and excited states of the cytosine radicals is studied by the CC singles and doubles (CCSD),[23–25] CCSD with noniterative triples correction [CCSD(T)] (Ref. 26), and EOM-CCSD (Ref. 27) methods. Besides applying EOM-CCSD to the cytosine H and OH adducts, these prototypical calculations, the largest of which employs 552 molecular orbitals and has no symmetry, serve to assess some performance aspects of the new parallel EOM-CCSD implementation in ACES III. The scalability of the program is gauged in the range from 32 to 256 processors, and timings of various size computations are reported. The program is coded in the superinstruction assembly language (SIAL) (details of the SIAL language and the execution of the SIAL program can be found in Ref. 28) as a part of the ACES III package.

II. THEORY AND COMPUTATIONS

The EOM-CC method forms the excited state wave function Ψ_k as

$$\Psi_k = R_k e^T |\phi_0\rangle. \tag{1}$$

Both R_k and T operators define the relation between the reference function ϕ_0 and the set of determinants $\{\mathbf{\Phi}\} = \{\phi_1, \phi_2, \ldots, \phi_n\}$,

[a]Electronic mail: kus@qtp.ufl.edu.

$$T|\phi_0\rangle = \sum_{i=1}^{n} t_i|\phi_i\rangle, \quad R|\phi_0\rangle = \sum_{i=0}^{n} r_i|\phi_i\rangle. \tag{2}$$

It is assumed here that T and R operators are defined within the same carrier space, as is the case in the majority of EOM-CC applications. However, in some variants of the EOM-CC method the basis of one operator differs from the basis of the other operator by a number of functions.[29,30]

After left-multiplication by e^{-T}, the Schrödinger equation for the kth excited state becomes

$$\bar{H}R_k|\phi_0\rangle = E_k R_k|\phi_0\rangle, \tag{3}$$

where the similarity transformed Hamiltonian $\bar{H}=e^{-T}He^{T}$ is constructed using the T operator determined from the set of nonlinear CC equations,

$$\langle\phi_i|\bar{H}|\phi_0\rangle = 0. \tag{4}$$

Projected from the left onto the $\{\mathbf{\Phi}\}$ space, Eq. (3) takes the form of the eigenvalue problem

$$\overline{\mathbf{H}}\mathbf{R}_k = E_k\mathbf{R}_k, \tag{5}$$

which one may transform so that the eigenvalues become the energies of the electron excitations from the reference level $\omega_k=E_k-E_0$,

$$(\overline{\mathbf{H}} - \mathbf{1}E_0)\mathbf{R}_k = \omega_k\mathbf{R}_k. \tag{6}$$

Since $\bar{H}$ is a non-Hermitian operator, its left-hand eigenvector is different from the right one, and the analogous eigenvalue equation needs to be solved whenever information about the left-hand eigenvector is required, typically for properties

$$\mathbf{L}_k(\overline{\mathbf{H}} - \mathbf{1}E_0) = \omega_k\mathbf{L}_k. \tag{7}$$

The left- and right-hand eigenvectors, although different, are chosen to be biorthogonal,

$$\langle\mathbf{L}_i|\mathbf{R}_j\rangle = \delta_{ij}. \tag{8}$$

If the reference function is a single determinant, the basis $\{\mathbf{\Phi}\}$ consists of the determinants created by interchanging some number of the occupied orbitals of the reference function by the unoccupied ones, which creates singly, doubly, and up to n-tuply excited determinants. The EOM-CCSD approximation limits the basis to singly and doubly excited configurations.

In the actual implementation of the EOM-CCSD method the diagonalization of the $\overline{\mathbf{H}}$ matrix is performed by a generalization of the Davidson diagonalization algorithm[31] to nonsymmetric cases.[32] The algorithm provides a number of the lowest solutions for the large matrix eigenvalue problem (the rank of the largest matrix diagonalized in the present study is approximately 5×10^9). The diagonalization scheme does not require creating the entire $\overline{\mathbf{H}}$ matrix but only the product between $\overline{\mathbf{H}}$ and an approximate vector $\mathbf{R}_k$. This enables a formulation of the EOM-CCSD equations that avoid directly creating the expensive three-body elements of $\overline{\mathbf{H}}$. For the same reason, the four-virtual elements of the similarity transformed Hamiltonian, which are the most numerous, can be constructed directly from atomic orbital integrals at every EOM iteration, as opposed to constructing the four-virtual $\overline{\mathbf{H}}$ elements from the molecular orbital integrals only once and storing them. Although the former strategy requires a larger number of floating-point operations, it reduces the storage significantly and, as shown in the subsequent part of the paper, increases the efficiency for large-scale computations. Both types of managing the four-virtual $\overline{\mathbf{H}}$ have been implemented and tested. The diagonalization algorithm applied requires assuming some value of a $\mathbf{R}_k$ vector at the first iteration. In the present implementation configuration interaction singles (CIS) vectors are used as the initial guess. The Hermitian CIS eigenvalue problem is solved by the Davidson procedure.

TABLE I. Timing results (in min/iteration) for cytosine H and OH adducts. First two results were obtained on the IBM p655+ supercomputer (using 128 processors), the others on the Sun Opteron cluster with 2.6 GHz AMD Opteron processors (using 256 processors).

	N_{occ} [b]	N_{tot} [c]	Time
1	22	246	6.7
2	25	270	9.5
3	22	506	10.5[a]
4	25	552	75.8

[a]The result obtained with a version of the program that avoids the storage of the four-virtual elements.
[b]The number of correlated occupied orbitals.
[c]The total number of correlated orbitals.

The C6 and C5 isomers of the OH cytosine adduct and the N3, C6, and C5 isomers of the H cytosine adduct are considered. Even though the OH and H additions to cytosine lead to more adducts than the ones considered here, theoretical results find that the other isomers have much higher energies[16,21,22] and, thus, are not expected to be formed in quantities large enough to contribute to the spectrum of a specific adduct. The equilibrium ground state geometries are optimized at the MBPT(2) level with the POL1 basis set[33] using the ACES III program package. The optimization is performed without any symmetry constraints and correlates all electrons. Using the obtained geometries, vertical excitation energies for all adducts are computed with the POL1 basis set. For the OH–C6 and H–N3 cytosine adducts excitation energies are also calculated with the aug-cc-pVTZ basis set.[34,35] The core electrons are frozen in all EOM-CCSD calculations. The unrestricted Hartree–Fock (UHF) reference function is used in the geometry optimization and EOM-CCSD calculations.

III. RESULTS

A. Parallel implementation

One of the performance aspects discussed in the present paper is the time for calculations. In Table I timings for the four computational problems of different sizes are collected. They correspond to vertical energy calculations for the H adduct with the POL1 basis set, OH adduct with POL1, H adduct with aug-cc-pVTZ, and OH adduct with aug-cc-pVTZ, respectively. Timings are calculated as the ratio of the total time of the $\overline{\mathbf{H}}$ diagonalization to the number of iterations required in the diagonalization. They do not include the

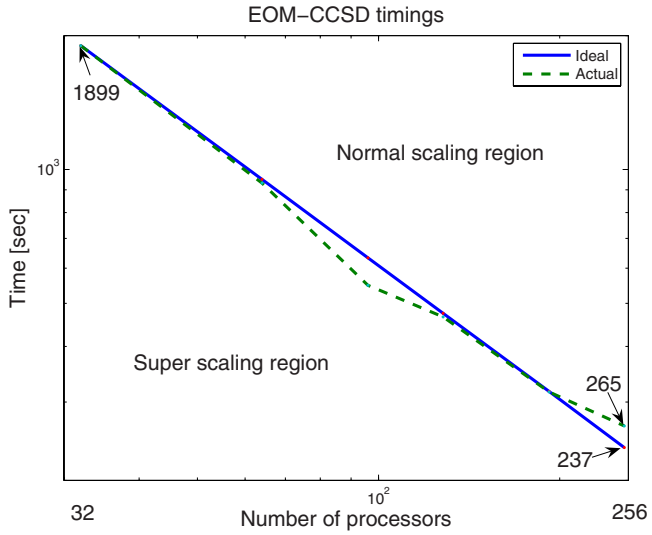

FIG. 1. (Color online) Time for one iteration of the EOM-CCSD program obtained using the IBM p655+ supercomputer.

CC ground state and CIS calculations, and the $\overline{\mathbf{H}}$ construction; the performance of the CC code is discussed elsewhere,[28] and the CIS calculations and $\overline{\mathbf{H}}$ construction are not rate determining factors as they take only a fraction of the total EOM-CCSD time. If more than one calculation of a particular size is performed, the corresponding timings are averaged.

An interesting aspect can be seen if one compares the two largest calculations performed with different variants of the program. If both calculations are performed with the same program, the timing ratio would be expected to be about 2. In fact, the obtained ratio is equal to 7.2, which indicates that the variant of the EOM-CCSD program used in the second case is faster by about 3.6. Hence, the version of the EOM-CCSD program that avoids storing any four-virtual elements is far more efficient, although it seems to be more computationally demanding due to the larger number of floating-point operations required. Such performance results from the large cost of I/O operations when there is an imbalance between the amount of I/O and computations. Evidently, this pertains to the EOM-CCSD calculations with the aug-cc-pVTZ basis set, which employ a large number of virtual orbitals and require creating a large number of four-virtual integrals and $\overline{\mathbf{H}}$ elements. For such a case increasing the amount of computations and decreasing the intensity of I/O by computing the same terms many times compared to computing them only once and retrieving them from the disk when needed help to achieve better performance.

Figure 1 presents timing results for the OH cytosine adduct with the POL1 basis set. The dimension of the computational problem is 25 occupied and 245 virtual orbitals. The timings presented are obtained using 32, 64, 96, 128, 192, and 256 processors, which permit a comparison with ideal scaling. The points obtained for 64, 128, and 192 processors show almost ideal scaling (98%, 98%, and 100% of the ideal time, respectively). The time for the 96 processor calculations is shifted into the superscaling region (87% of the ideal time), and the time for the 256 processor calculations is placed in the normal scaling region (112% of the ideal time). Taking into account that up to 192 processors the scaling for all points but one is virtually perfect, it is very likely that the deviation for 96 processors was caused by a fluctuation in the machine performance, which became more efficient during the 96 processor calculations. The increase in the calculation time for 256 processor computations results from too small a size of the computational problem to keep all 256 processors busy.

B. Relative energies of isomers

The structures of the cytosine molecule and five cytosine adducts are shown in Fig. 2. The MBPT(2) optimized geometry of the cytosine molecule was already published by Sponer and Hobza.[36] Since the largest basis sets used there are expected to yield similar accuracy as our computations, the main goal of the cytosine calculations is to verify the accuracy level by comparison with the experimental data, which are not available for cytosine adducts. It should be noted that the experimental data, consisting of the bond lengths and angles between heavy atoms, are obtained by analysis of the x-ray determined structures of 14 compounds containing cytosine;[37] thus, good agreement with the values computed for the cytosine molecule in a vacuum is not expected. The average of absolute deviations from the experimental values is equal to 0.019 Å for the MBPT(2)/POL1 study. The analogous values are equal to 0.014 and 0.018 Å at the mutliconfiguration self-consistent -field (MCSCF/CEP-31G) (Ref. 15) and density-functional theory [DFT/B3LYP/6-31+G(d,p)] (Ref. 21) levels of theory, respectively.

The comparison of the structural data provided by the EOM method with other theoretical results shows that DFT values are more consistent with EOM than are the MCSCF data. For both OH isomers the average of the absolute discrepancies between the MCSCF and EOM-CCSD values is equal to 0.011 Å. The same values for the DFT/UB3LYP/6-31G(d,p) study of Ji *et al.*,[16] where only a limited number of parameters are cited, are equal to 0.005 and 0.006 Å for the C6 and C5 isomers, respectively. The MCSCF geometries of H adducts deviate from MBPT(2) results by 0.021, 0.013, and 0.014 Å for the N3, C5, and C6 isomers, respectively, with DFT results being closer to the MBPT(2) ones. The average values of the absolute deviations between MBPT(2) and the results provided by the DFT study of Turecek and Yao[21] and DFT/B3LYP/DZP++ results of Zhang *et al.*[22] fall between 0.003 and 0.008 Å.

For the relative stability of the isomers, the MCSCF/CEP-31G (Ref. 15) and DFT/UB3LYP/6-31++G(d,p) (Ref. 16) results determine the C6–OH isomer to be more stable than the C5 one (19 and 5.3 kJ/mol, respectively). The experimentally observed preference of the OH addition to the C5 site[7] suggests the presence of a small energy barrier for the C6 adduction, whereas the C5 adduction has no such barrier.[16] CCSD/POL1 energies calculated at MBPT(2) optimized geometries show a negligible energy difference between the C6 and C5 isomers of −0.6 kJ/mol. Because of such a small energy difference we have performed additional calculations in order to determine the impact of the basis set

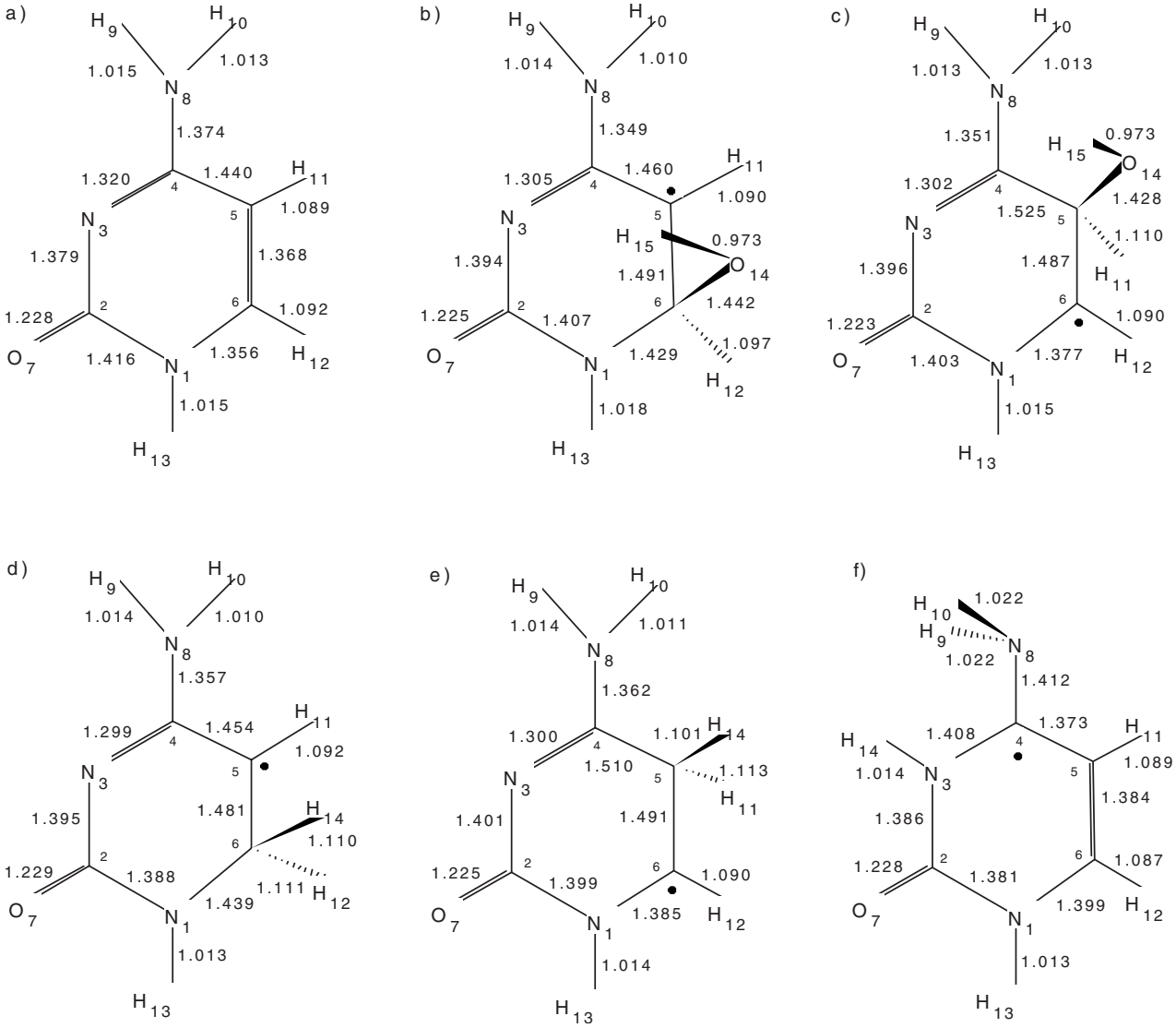

FIG. 2. The ground state geometries of the cytosine molecule (a), and OH [(b) and (c)], and H [(d), (e), and (f)] cytosine adducts. The bond lengths are in angstrom. Details of the optimization are in the text.

quality and correlation treatment on the relative energies of the isomers. The results are presented in Fig. 3. They indicate that an improvement in the calculations from MBPT(2) to CCSD and CCSD(T), and basis set from POL1 to aug-cc-pVTZ, has little effect on the energy difference. All values predict the C6 isomer to be slightly more stable with values oscillating between 0.6 and 3.1 kJ/mol. Such small differences are likely to have a much smaller influence on the adduction preference then other thermodynamical factors, which can cause the C5 adduction to be favored. These CC results agree better with the DFT/UB3LYP/6-31++G(d,p) (Ref. 16) study than with the MCSCF results. In the case of the CCSD(T) calculations using the aug-cc-pVTZ having 552 functions, ACES III took 7500–8400 s for CCSD with 1000 processors, while (T) took about 28 000 s.

The N3–H adduct has the lowest energy among the H cytosine adducts with the C5 and C6 isomers located 17.0 and 31.8 kJ/mol above it, respectively. However, while all other methods show that the N3–H adduct is the most stable, the energy differences are larger than those calculated by the EOM-CCSD method. MCSCF results locate the C5 and C6 isomers, respectively, 26 and 24 kJ/mol above the N3 one. In this study the C5 adduct is more stable than the C6 one, unlike in all other theoretical studies. The DFT/B3LYP/6-31+G(d,p) calculations of Turecek and Yao[21] yield the relative energies of the C5 and C6 isomers with respect to the N3 isomer equal to 31 and 37 kJ/mol, respectively, while the corresponding DFT/B3LYP/DZP++ results of Zhang *et al.*[22] give 26.4 and 35.1 kJ/mol.

C. Numerical results for excited states of cytosine adducts

Vertical excitation energies calculated with the EOM-CCSD method are presented in Table II. For each isomer the excitation energies to the five lowest excited states are reported. All these states are doublets. In order to get more insight into the intensity of transitions considered, the oscillator strengths are computed using the CIS method with POL1 basis set. Since all excited states considered are singly excited character states, CIS approximation is expected to

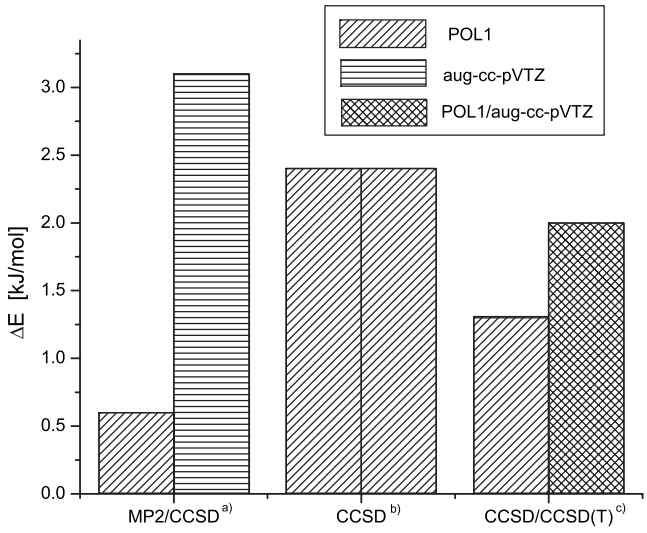

FIG. 3. Relative stability of the C6– and C5–OH cytosine adducts presented as $\Delta E = E_{C5} - E_{C6}$ (in kJ/mol) at various levels of theory. (a) CCSD energies calculated at the MBPT(2) geometry. (b) CCSD energies calculated at the CCSD geometry. (c) CCSD(T) energies calculated at the CCSD geometry; the first bar presents values obtained with the POL1 basis set; the second, CCSD(T)/aug-cc–pVTZ energies calculated at the CCSD/POL1 geometries.

provide qualitatively correct results for transition moments. In all calculations the UHF reference function is used. At the SCF level, the largest spin contamination occurs for the N3–H adduct, where the S^2 expectation value is equal to 0.93. For the other radicals the S^2 expectation value oscillates between 0.77 and 0.83. Such a nonsignificant spin contamination of the ground states, which is subsequently extensively reduced by the CCSD correction,[38] is not expected to introduce errors larger than 0.1 eV at the EOM level.

Let us focus on OH adducts first. For the C6–OH isomer, oscillator strengths indicate that the two states are of greatest interest. These are the first and fourth excited states having oscillator strengths equal to 0.081 and 0.009, respectively. The lowest one arises by exciting an electron from the highest occupied beta-spinorbital into the lowest unoccupied beta-spinorbital. The fourth excited state has more diffuse character. The leading configurations are formed by exciting an electron into the lowest unoccupied beta-spinorbital from orbitals lying below the highest occupied orbital. Three excited states of the C5–OH adduct are expected to have considerable intensities. The first, second, and fourth excited states have oscillator strengths equal to 0.021, 0.009, and 0.036, respectively. For all these states an electron is promoted from the singly occupied orbital.

The effect of improving the basis set quality turns out to be relatively small. The excitation energy differences between the aug-cc-pVTZ and POL1 basis sets for the three lowest excited states of the C6–OH adduct are equal to 0.04, 0.00, and 0.06 eV, respectively. The tendency to increase the excitation energy with improving basis set is consistent with the MCSCF results. MCSCF excitation energies increase by a value between 0.11 and 0.34 eV when the DZ basis set is replaced by POL1.

The comparison of EOM-CCSD results with the experimental data, which is possible for the OH adducts, has to be conducted carefully since the experimental absorption spectrum is measured in a water environment.[12] The two experimental broad absorptions have their maximum peaks at 2.88 and 3.65 eV. Krauss and Osman[15] attempted to assign the calculated vertical excitation energies to the observed absorptions by computing the oscillator strengths and dipole moments of some excited states. Dipole moment calculations are used to estimate the blueshift in water. Their results predict that the two lowest transitions of the C6 isomer contribute to the lower energy absorption, while the third transition of the C6 isomer and the two lowest transitions of the C5 adduct contribute to the second absorption. The MCSCF blueshifts for the C6–OH isomer indicate that the average blueshift is equal to about 0.05 eV and predict that the second excited state is the dominant contributor because of its larger oscillator strength. Our calculations identify the first transition as the dominant one since the CIS oscillator strength is 0.081 for this state, as opposed to 0.003 for the second one. The MCSCF results predict the second transition of the C5 adduct as the main contributor to the second absorption. Four EOM states of the OH adducts are located in the region of the second absorption peak. These are the third and fourth states of the C6–OH adduct and the first and second states of the C5–OH isomer. Among these states, the first and second states of the C5–OH isomer and the fourth state of the C6–OH adduct have considerable oscillator strengths. The excitation energy of the second state of C5–OH isomer, after assuming 0.1 eV blueshift, is located about 0.5 eV above the experimentally observed peak; the two other excitation energies are much closer to the experimental value. Thus, EOM-CCSD results agree with MCSCF data that the first absorption of the C5–OH isomer (which appears as the second one in MCSCF calculations) is dominant but also point out that the fourth excited state of the C6–OH radical contributes to the second experimentally observed absorption.

TABLE II. Vertical excitation energies (in eV) for cytosine H and OH adducts; the MBPT(2)/POL1 optimized geometry is used.

Isomer	Method	1	2	3	4	5
OH–C6	EOM/POL1	2.63	2.92	3.39	3.64	4.62
	EOM/pVTZ+	2.67	2.92	3.45		
OH–C5	EOM/POL1	3.71	4.00	4.32	4.47	4.50
H–C6	EOM/POL1	2.87	3.05	3.33	3.79	5.23
H–C5	EOM/POL1	3.56	3.75	4.30	4.51	4.66
H–N3	EOM/POL1	2.94	2.97	3.39	3.99	4.03
	EOM/pVTZ+	2.98	3.14	3.56	4.14	4.15

The excited states of C6–H radical of considerable oscillator strength are similar to the C6–OH ones. They also involve excitations from the highest beta-spinorbitals. The C5–H and N3–H adducts exhibit the largest oscillator strengths for the first and fifth excited states. Their leading configurations resemble those of C5–OH radical as the excitations from the singly occupied orbital are engaged.

The comparison of vertical excitation energies of the three H adducts shows that the distribution of excited state energy levels for the C6–H and N3–H adducts is similar to the C6–OH isomer. Interestingly, for N3–H radical this similarity is not reflected by the excited states themselves, which are resembling the C5-H and –OH isomers. The similarities can be observed between both excitation energies and wave functions of the C5–H and C5–OH radicals. This is consistent with theoretical anticipation based on the analysis of the structures and bond types, which leads to the conclusion that C6–OH, C6–H, and N3–H adducts should possess lower lying excited states than the C5–OH and C5–H adducts.[15]

EOM-CCSD calculations support the observation of Krauss and Osman[15] that the similarity in the distribution of excited state energy levels makes it very difficult to distinguish the corresponding OH and H adducts by the analysis of the spectra. For the C5–H and –OH adducts, the first and fifth transitions have significant oscillator strengths of about 0.02 and 0.03, respectively. The differences in excitation energies between the corresponding states are smaller than 0.2 eV. The lowest transitions of the C6–OH, C6–H, and N3–H adducts, all of them of substantial oscillator strengths, are also located very close to each other (2.63, 2.87, and 2.94 eV, respectively). Larger differences can be observed for the second absorption of a considerable oscillator strength. These are the fourth state of C6–OH, the third state of C6–H, and the fifth state of N3-H, which have excitation energies equal to 3.64 (0.009), 3.33 (0.012), and 4.03 eV (0.038), respectively, with the oscillator strengths given in parentheses.

The differences between the POL1 and aug-cc-pVTZ basis sets computed for the N3–H adduct are larger than the corresponding values calculated for the C6–OH adduct. The energy is also increased, but the effect is larger, with the average differences being equal to 0.13 eV. The largest discrepancies between the MCSCF and EOM-CCSD methods occur for the C6–H adduct where the MCSCF method overestimates EOM-CCSD values by 0.36 and 0.39 eV for the two lowest excited states, respectively. For the N3–H isomer the MCSCF energy also overestimates the corresponding EOM-CCSD value, while for the C6–H adduct all results but one are underestimated.

IV. CONCLUSIONS

Results of the EOM-CCSD ACES III parallel implementation show performance that encourages further applications and developments. The calculations using 32, 64, 96, 128, 192, and 256 processors determine the scaling of the program, which appears to be very close to ideal. The performance of calculations involving 506 molecular orbitals indicates that carrying out 100 iterations, which usually allows convergence from 5 to 6 eigenstates, takes 17.5 h on 256 processors. These observations create an opportunity to apply the EOM-CCSD method to much larger systems than was possible before and, thus, allow for excited state CC calculations for molecules of biological interest.

The first application of the program is the study of vertical excitation energies of the five most important cytosine radicals involved in processes of DNA damage. These open-shell molecules have no symmetry to simplify the calculations. Our computations, which employ larger basis sets than the preceding studies, provide data that in many points are consistent with previous experimental and theoretical findings. In some cases, as the relative stability of OH adducts, or the assignment of the second absorption, our results differ from the previous ones.

ACKNOWLEDGMENTS

The project was supported by the U.S. Air Force Office of Scientific Research under Contract No. FA-9550-04-1-01. Besides the authors, the ACES III team includes Dr. Erik Deumens, Dr. Norbert Flocke, Dr. Ajith Perera, and Mr. Mark Ponton, whose contributions are critical to the development of the program. We would also like to thank the Arctic Region Supercomputer Center consultants for their support in testing and developing our program.

[1] C. von Sonntag, *Chemical Basis of Radiation Biology* (Taylor and Francis, London, 1987).
[2] *Advances in Cell Aging and Gerontology*, edited by B. A. Gilchrest and V. A. Bohr (Elsevier, New York, 2001), Vol. 4.
[3] Y. Jin, F. J. Burns, S. J. Garte, and S. Hosselet, Carcinogenesis **17**, 873 (1996).
[4] K. B. Beckman and B. N. Ames, Physiol. Rev. **78**, 547 (1998).
[5] M. Valiev and K. Kowalski, J. Chem. Phys. **125**, 211101 (2006).
[6] E. Epifanovsky, K. Kowalski, P.-D. Fan, M. Valiev, S. Matsika, and A. I. Krylov, J. Phys. Chem. A **112**, 9983 (2008).
[7] D. K. Hazra and S. Steenken, J. Am. Chem. Soc. **105**, 4380 (1983).
[8] H. Catterall, M. J. Davies, B. C. Gilbert, and N. P. Polack, J. Chem. Soc., Perkin Trans. 2 **2039** (1993).
[9] C. Hazlewood and M. J. Davies, J. Chem. Soc., Perkin Trans. 2 **895** (1995).
[10] L. S. Myers, Jr., M. L. Hollis, L. M. Theard, F. C. Peterson, and A. Warnick, J. Am. Chem. Soc. **92**, 2875 (1970).
[11] E. Hayon and M. Simic, J. Am. Chem. Soc. **95**, 1029 (1973).
[12] A. Hissung and C. von Sonntag, Z. Naturforsch. **88b**, 321 (1978).
[13] A. O. Colson, D. Becker, I. Eliezer, and M. D. Sevilla, J. Phys. Chem. A **101**, 8935 (1997).
[14] S. D. Wetmore, F. Himo, R. J. Boyd, and L. A. Eriksson, J. Phys. Chem. B **102**, 7484 (1998).
[15] M. Krauss and R. Osman, J. Phys. Chem. A **101**, 4117 (1997).
[16] Y. J. Ji, Y. Y. Xia, M. W. Zhao, B. D. Huang, and F. Li, J. Mol. Struct.: THEOCHEM **723**, 123 (2005).
[17] W. Wang and M. D. Sevilla, Radiat. Res. **138**, 9 (1994).
[18] J. Ohlmann and J. Huttermann, Int. J. Radiat. Biol. **63**, 427 (1993).
[19] C. Yao, F. Turecek, M. J. Polce, and C. Wesdemiotis, Int. J. Mass Spectrom. **265**, 106 (2007).
[20] Y. Huang and H. Kenttämaa, J. Am. Chem. Soc. **125**, 9878 (2003).
[21] F. Turecek and C. Yao, J. Phys. Chem. A **107**, 9221 (2003).
[22] J. D. Zhang, Y. Xie, H. F. Schaefer III, Q. Luo, and Q.-S. Li, Mol. Phys. **104**, 2347 (2006).
[23] G. D. Purvis III and R. J. Bartlett, J. Chem. Phys. **76**, 1910 (1982).
[24] R. J. Bartlett, Annu. Rev. Phys. Chem. **32**, 359 (1981).
[25] R. J. Bartlett, C. E. Dykstra, and J. Paldus, in *Advanced Theories and Computational Approaches to the Electronic Structure of Molecules*, edited by C. E. Dykstra (Reidel, Dordrecht, 1983).
[26] K. Raghavachari, G. W. Trucks, J. A. Pople, and M. Head-Gordon, Chem. Phys. Lett. **157**, 479 (1989).
[27] H. Sekino and R. J. Bartlett, Int. J. Quantum Chem., Quantum Chem.

Symp. **18**, 255 (1984).
[28] V. Lotrich, N. Flocke, M. Ponton, A. D. Yau, A. Perera, E. Deumens, and R. J. Bartlett, J. Chem. Phys. **128**, 194104 (2008).
[29] S. Hirata, M. Nooijen, I. Grabowski, and R. J. Bartlett, J. Chem. Phys. **114**, 3919 (2001).
[30] L. V. Slipchenko and A. I. Krylov, J. Chem. Phys. **123**, 084107 (2005).
[31] E. R. Davidson, J. Comput. Phys. **17**, 87 (1975).
[32] K. Hirao and H. Nakatsuji, J. Comput. Phys. **45**, 246 (1982).
[33] A. Sadlej, Theor. Chim. Acta **79**, 123 (1991).
[34] T. H. Dunning, Jr., J. Chem. Phys. **90**, 1007 (1989).
[35] R. A. Kendall, T. H. Dunning, Jr., and R. J. Harrison, J. Chem. Phys. **96**, 6796 (1992).
[36] J. Sponer and P. Hobza, J. Phys. Chem. **98**, 3161 (1994).
[37] R. Taylor and O. Kennard, J. Mol. Struct. **78**, 1 (1982).
[38] G. D. Purvis III, H. Sekino, and R. J. Bartlett, Collect. Czech. Chem. Commun. **53**, 2203 (1988).